CHALMERS

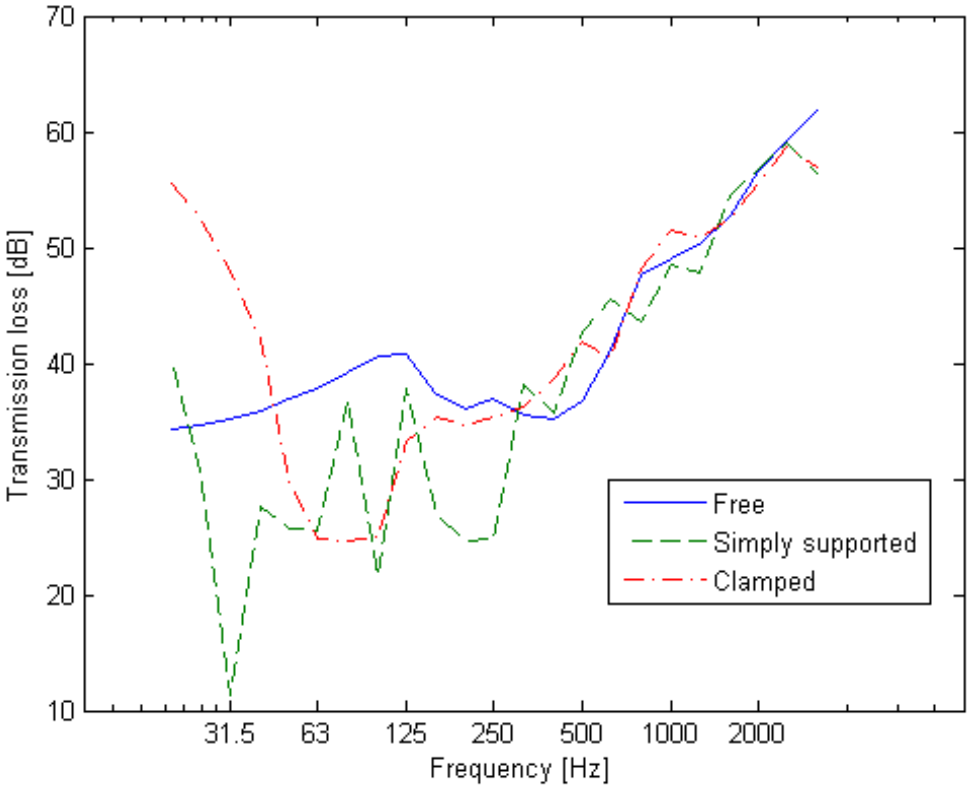

The influence of Boundary Conditions on Sound Insulation

Master's Thesis in the Master's programme in Sound and Vibration

CHRISTOFFER JANCO

Department of Civil and Environmental Engineering
Division of Division of Applied Acoustics
Vibroacoustics Group
CHALMERS UNIVERSITY OF TECHNOLOGY
Göteborg, Sweden 2012
Master's Thesis 2012:51

MASTER'S THESIS 2012:51

The influence of Boundary Conditions on Sound Insulation

Master's Thesis in the Master's programme in Sound and Vibration

CHRISTOFFER JANCO

Department of Civil and Environmental Engineering
Division of Division of Applied Acoustics
Vibroacoustics Group
CHALMERS UNIVERSITY OF TECHNOLOGY

Göteborg, Sweden 2012

The influence of Boundary Conditions on Sound Insulation
Master's Thesis in the Master's programme in Sound and Vibration
CHRISTOFFER JANCO

Master's Thesis 2012:51
Department of Civil and Environmental Engineering
Division of *Applied Acoustics*
Vibroacoustics *Group*
Chalmers University of Technology
SE-412 96 Göteborg
Sweden
Telephone: + 46 (0)31-772 1000

Cover:
Calculated transmission loss of a lightweight concrete wall for three different boundary conditions. See section 5.1 for more extensive information.

Printed by:
Chalmers reproservice
Göteborg, Sweden 2012

The influence of Boundary Conditions on Sound Insulation

Master's Thesis in the Master's programme in Sound and Vibration

CHRISTOFFER JANCO
Department of Civil and Environmental Engineering
Division of Division of *Applied Acoustics*
Vibroacoustics Group
Chalmers University of Technology

ABSTRACT

When measuring the sound reduction index of equal construction elements in different laboratories the results often differ from one another. The discrepancies are due to many factors concerning the laboratory design. A lot of these factors have been thoroughly studied but the dependence upon some factors is still not fully understood. A rather neglected aspect is the influence that the mounting of a wall has on the sound insulation. This thesis is based on the hypothesis that the boundary conditions, i.e. the mechanical properties of the mounting, of a partition have a considerable effect on the sound insulation. The diffuse field transmission loss of three different single panel walls is modelled for different boundary conditions. The wall is excited by plane waves and the radiation is calculated using the Rayleigh integral. The diffuse field transmission loss is obtained by averaging the transmission loss for a number of angles of incidence. The results show that the transmission loss has a large dependence on the boundary conditions and that walls having close to free boundaries have the best sound insulation properties.

Key words: Sound Insulation, Sound Transmission, Boundary Conditions

Contents

1 Introduction

In the field of building acoustics the sound insulation of partitions is commonly described by the sound reduction index which is a measure of the attenuation of diffuse field sound energy between two rooms. Sound reduction measurements are carried out both in laboratories and in field. Measurements of partitions in buildings give the energy transmission between two rooms including flanking transmission and losses to adjacent walls and floors whereas these effects are avoided or at least minimized in laboratories. When measuring the sound reduction index of a construction element in different laboratories the results often differ from one another. The discrepancies are due to many factors concerning the laboratory design, e.g. flanking transmission and niche effects.

In most countries there are strict standardized regulations concerning the sound insulation between dwellings and it is therefore necessary to know how different parameters influence the sound insulation. Laboratory measurements of wall constructions are often used as reference to make sure that the sound insulation fulfils the conditions specified in the regulations.

As a rule of thumb it can be said that laboratory testing gives a 3 dB higher sound insulation compared to measurements in field (swedish standard SS 25267). Field measurements typically result in 3 – 4 dB lower sound insulation given that the construction is optimally designed and built considering flanking (Gyproc Handbook). With minimized flanking there is still an increase of sound transmission which is known through experience but not theoretically explained.

If the mounting of a wall in a building differs from that of the reference measurement there is a risk that the wall construction does not fulfil the requirements. As long as these effects are not fully understood there will always be a risk that buildings are incorrectly designed and that measures have to be taken after the building is completed which will of course be more time consuming and expensive.

This thesis is based on the hypothesis that the boundary conditions, i.e. the mechanical properties of the mounting, of a partition have a considerable influence on the sound insulation. If the boundary conditions prove to have substantial influence on the sound insulation it may be of practical interest to investigate how careful mounting of walls can increase the sound reduction.

Background

The effects of boundary conditions on sound insulation are not as elucidated as the effects of other properties such as mass and stiffness of single panel partitions and distance between panels for multi-layer partitions. One reason for this may be that it is not possible to find a general formulation describing the dependence for arbitrary wall dimensions and boundary conditions. Another reason may be that the boundary effects have not shown to be of great importance compared to other properties of the partition or that the

question may not have been asked at all. However, the stiffness of mountings does not seem to be negligible as has been shown by Kihlman & Nilsson (1972). Kihlman and Nilsson compared the sound reduction indices of lightweight concrete walls having firm and elastic mountings. The boundary conditions were not rigorously evaluated but the results show that the firm mounting gave a lower sound reduction index compared to the elastic mounting. Kihlman and Nilsson's study concerns the sound reduction index in the frequency range 100-3150 Hz while there is reason to believe that the influence of the boundary conditions is even greater at lower frequencies around the first resonances of the wall which may be of great interest when the sound source is for example music or traffic noise.

Below the critical frequency where the free bending wavelength on the wall is shorter than the wavelength in air the sound transmission can be divided into forced and resonance transmission. Above the critical frequency the transmission is governed by the coincidence effect which is a type of resonance phenomenon and the division in forced and resonance transmission loses its relevance. Forced transmission is said to follow infinite panel theory (Kihlman & Nilsson 1972, Sewell 1970) while resonance transmission is the result of excitation of and radiation from resonant modes on the wall. Since both excitation and radiation of structural modes is proportional to the radiation efficiency of a wall (Fahy et al. 2007, p. 294), sound transmission is very closely related to radiation efficiency. The radiation efficiency of rectangular plates has been studied in many papers, e.g. Maidanik (1962) and Smith (1964). At subcritical frequencies above the first resonance frequency, twice as much power radiates from clamped plates compared to simply supported plates (Smith 1964). Numerical studies by Berry et al. (1990) show that free plates radiate less than both simply supported and clamped plates. Considering resonance transmission both excitation and radiation is proportional to the modal radiation efficiency which is why the ratio of forced transmission to resonance transmission is inversely proportional to the modal averaged radiation efficiency squared (Fahy & Gardonio 2007).

According to Nilsson (1972) and Sewell (1970) the subcritical transmission loss is lower for clamped walls compared to simply supported walls and Sewell's results show that the free wall has the highest transmission loss which is explained by negligible resonance transmission.

Sewell's results show that the transmission loss above the critical frequency is independent of boundary conditions which is also claimed by Kihlman and Nilsson (1972) with the exception that edge damping may play a significant role. In more recent numerical studies it is claimed that the influence of rotational stiffness is negligible compared to translational stiffness concerning both radiation efficiency (Berry et al. 1990) and transmission loss (Chiello et al. 2003).

Purpose of study

The aim of this master's thesis project is to investigate how the sound insulation of single panel partitions of common building materials is influenced by translational and rotational stiffness at the edges. The response of a baffled plate to a diffuse field is modelled using commercial FEM software and the sound power radiating from the vibrating plate is obtained from a numerical model based on the Rayleigh integral.

2 Theory

Longitudinal and transversal waves are the two fundamental wave types that appear in solids. Bending waves is generally the most interesting wave type when it comes to sound due to their transversal displacement.

2.1 Bending waves in plates

For a plate in the xy – plane with displacement η perpendicular to the surface the bending wave equation is

$$D\left(\frac{\partial^4\eta}{\partial x^4}+2\frac{\partial^2\eta}{\partial x\partial y}+\frac{\partial^4\eta}{\partial y^4}\right)+m''\frac{\partial^2\eta}{\partial t^2}=0 \tag{2.1}$$

where m'' is the mass per unit area and D is the bending stiffness. The phase speed of the wave is frequency dependent and is given by

$$c_B=\sqrt[4]{\frac{D}{m''}\omega^2} \tag{2.2}$$

At a certain frequency the phase speed of the bending waves on the plate coincides with the longitudinal phase speed in air. This frequency is called the critical frequency and is obtained by substituting the left hand side of equation (2.2) by the speed of sound in air

$$f_c=\frac{c^2}{2\pi}\sqrt{m''/D} \tag{2.3}$$

The vibration field of bending waves is often fairly complicated since, in addition to propagating waves, also near-field waves arise at discontinuities and contribute to the displacement.

2.2 Sound radiation from free bending waves on plates

As has been shown above, the phase speed of bending waves is dependent upon frequency. At low frequencies the bending wavelength is shorter than the wavelength in air which, for an infinite plate, causes acoustic cancellation between volumes of positive and negative pressure. At the critical frequency the wavelength in air and the wavelength on the plate are matched. At and above the critical frequency sound radiates from a vibrating infinite plates. Below the critical frequency no sound is radiating from an infinite plate. However, all real life plates are finite and sound does radiate even below the critical frequency from the edges of the plate or other discontinuities where acoustic cancellation is not complete. The sound radiation at the edges depends on the shape of the vibrations and therefore to a large extent on the boundary conditions.

Mathematically the concept of sound radiation can be described using wave numbers. Consider a sound wave radiating from a plate on which a bending wave is propagating only in the x-direction. The wave number k=ω/c of a sound wave can for a two dimensional problem be decomposed in its x- and z-components where the z-axis is normal to the plate. The relation between the components is

$$k^2 = {k_x}^2 + {k_z}^2 \tag{2.4}$$

The x-component of the acoustic wave number must equal the wave number κ of the bending wave so the spatial variation along the z-axis is given by

$${k_z}^2 = k^2 - \kappa^2 \tag{2.5}$$

The velocity of the fluid and the plate in the z-direction must be equal at the interface and by using the fluid momentum equation the sound pressure in the positive half-space is given by (Cremer et al.)

$$p(x,z) = \frac{\rho c \hat{v}}{\sqrt{1-\kappa^2/k^2}} \mathrm{e}^{-\mathrm{j}\kappa x - j\sqrt{k^2-\kappa^2}z} \tag{2.6}$$

where $\hat{v}$ is the plate velocity amplitude. Equation (2.6) is valid as long as the bending wavelength is longer than the acoustic wavelength, i.e. $\kappa < k$. When the bending wavelength is shorter the pressure amplitude is exponentially decreasing with z and no pressure wave is propagating to the far field.

$$p(x,z) = j\frac{\rho c \hat{v}}{\sqrt{\kappa^2/k^2-1}} \mathrm{e}^{-\mathrm{j}\kappa x - \sqrt{k^2-\kappa^2}z} \tag{2.7}$$

At the critical frequency, i.e. where $\kappa = k$, the fluid impedance and consequently the sound pressure is theoretically infinite which cannot occur in practice since all plates are finite. For all angles from the normal to the plate, there is one frequency for which the x-component of the acoustic wave number and the bending wave number are matched as is depicted in figure 2.1. This angle dependent frequency is called the coincidence frequency.

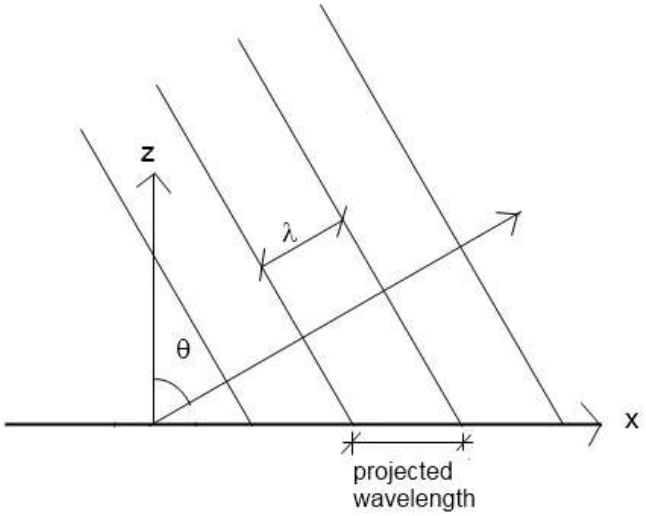

Figure 2.1 Plane sound wave and plate, oblique incidence.

The geometrical relation between incident plane waves and bending waves on a plate is applicable for studies of both excitation and radiation problems. To extend the analysis to three dimensions a coordinate system need to be defined. Let the origin of the coordinate system be in the middle of the plate and let each point in the half space above the plate be determined by the distance R to the origin and the angle θ from the normal of the plate and φ on the xy-plane, frequently referred to as the colatitude and the longitude coordinate respectively considering spherical coordinates in mathematics. The coordinate system is depicted in figure 2.2.

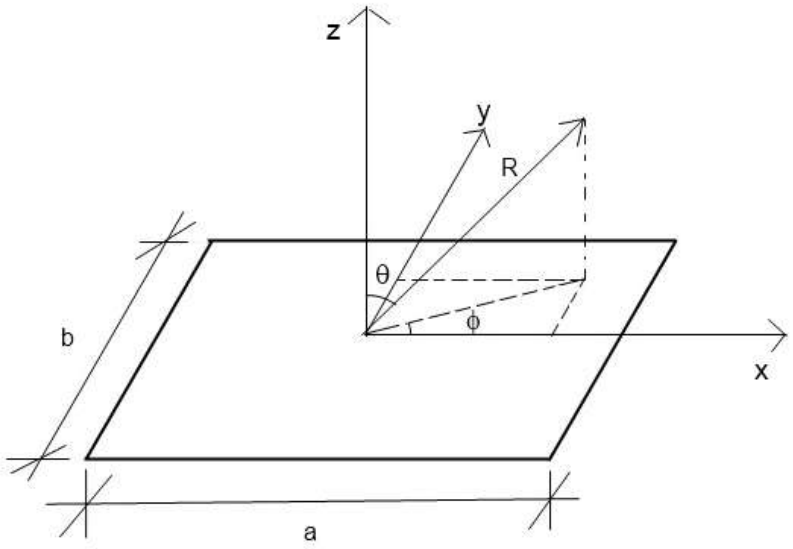

Figure 2.2 Coordinate system centred at centre of a plate with length a and width b.

The trace wave numbers on the plate are

$$k_x = k \sin\theta \cos\phi \qquad k_y = k \sin\theta \sin\phi \tag{2.8}$$

2.3 Sound radiation from bending waves on finite plates

For an infinite plate without impedance discontinuities the wavelength on the plate equals that of the projected plane wave. However, for a finite plate the boundaries present discontinuities which distorts the shape of the vibration.

One way to analyze the radiation from a plate is to study the vibration in a wave number spectrum by making a Fourier transform in the spatial domains in the same manner as frequency spectra are obtained from the time domain. Considering free vibration of an infinite plate, the shape of the vibration is simply given by the bending wave number associated with that frequency and the wave number spectrum is simply a point at that wave number. However, for finite plates the vibrations are scattered at the boundaries deforming the vibration into a spectrum of wave numbers. The power radiating to the far field is obtained by integrating the squared velocity of the wave number spectrum from zero to the wave number of the critical frequency and multiplying it with some constants.

2.4 Radiation efficiency

Radiation efficiency is defined as the ratio of the sound power radiating from a vibrating plate to the power carried by a plane wave having rms velocity equal to the space averaged mean squared velocity of the plate and identical surface area.

$$\sigma = \frac{P_{rad}}{S\rho c\langle v^2 \rangle} \tag{2.9}$$

where P_{rad} is the actual radiating power, S the surface area of the plate, ρc the characteristic impedance of air and $\langle v^2 \rangle$ is the space averaged mean squared velocity. The radiation efficiency for free bending waves on an infinite plate equals zero below the critical frequency and goes to infinity at the critical frequency and approaches unity immediately above. If an infinite plate is excited by a plane wave incident at angle θ from the normal of the plate, the radiation efficiency equals sec (θ) (Fahy & Gardonio 2007). Above the critical frequency the radiation efficiency is approximately unity and is independent of the type of excitation (Cremer et al. 2005).

In consecutive sections of this text, all radiation efficiency plots will give the logarithmic value $10 \log_{10} \sigma$.

2.5 Single panel transmission loss

When sound is incident upon a surface of a partition it induces vibration which in turn causes radiation of sound. The ratio of the radiating sound power on the opposite side of the partition to the incident sound power defines the transmission coefficient.

$$\tau = \frac{W_{rad}}{W_{in}} \tag{2.10}$$

Transmission loss describes how much of the sound power incident on a partition that is prevented from propagating through the partition and is defined as

$$TL = 10\log\left(1/\tau\right) \tag{2.11}$$

In the field of building acoustics, sound insulation is generally defined as diffuse field transmission loss. In a diffuse field there is an equal probability that sound waves are incident at any angle and the phase is random. An approximate diffuse field is attainable in a room, but grazing incidence, i.e. waves propagating parallel to a surface, does not occur in practice and it has been empirically concluded by comparing theory to experimental results that a "diffuse" sound field contains sound waves arriving at angles between 0° and 78° from the normal, often referred to as field incidence (Fahy & Gardonio 2007).

Below the first resonance frequency of the panel the sound transmission depends on the stiffness of the mountings and the transmission loss decreases approximately 6 dB per octave. Above the first panel resonance the transmission loss can be approximated according to the equations below which are based on infinite plate theory. Below the critical frequency the transmission loss depends on the mass of the panel and increases 6 dB per octave and can be approximated as (Fahy & Gardonio 2007)

$$TL_D = 20\log_{10}(fm'') - 47 \tag{2.12}$$

which is called the mass law. At the critical frequency the mass and stiffness parts of the impedance cancels each other and the transmission loss is therefore dependent upon damping and the transmission loss can be approximated as (Forssén & Hornikx 2010)

$$TL_D = 20\log_{10}(fm'') + 10\log_{10}(\eta) - 39 \tag{2.13}$$

Above the critical frequency the transmission loss is stiffness controlled and increases 9 dB per octave. The transmission loss can be approximated as (Fahy & Gardonio 2007)

$$TL_D = 20\log_{10}(fm'') + 10\log_{10}\left(\frac{f}{f_c} - 1\right) + 10\log_{10}(\eta) - 49 \tag{2.14}$$

The mechanisms that control sound transmission are rather complex. The

sound transmission through a finite panel can be divided into forced transmission according to infinite panel theory and resonant transmission which is the transmission due to resonant modes. Kihlman and Nilsson (1972) argue that below the critical frequency the forced transmission follows the mass law while the resonant transmission depends on excitation of vibration modes and the modal sound radiation from the edges of the panel. The total sound transmission is a combination of both these phenomena. Since both modal excitation and radiation depends on the radiation efficiency the resonant transmission depends on the area and the perimeter of the partition as well as the boundary conditions. However, both theoretical analysis and experimental results show that the forced-wave process tends to transmit more energy than the resonant process (Fahy & Gardonio 2007). Above the critical frequency, diffuse field transmission is governed by the coinciding waves. Since the coincidence phenomenon can be interpreted as a type of resonance the transmission loss is to a large extent dependent upon damping (Kihlman, T. 1970).

2.6 Sound reduction index

In order to facilitate the comparison of sound insulation for different constructions standardized single number quantities have been developed. A measured or calculated transmission loss spectrum is compared to a standardized reference curve in order to obtain a weighted sound reduction index, R_w. Additional spectrum adaption terms may be calculated in order to take low frequencies into account and to assess sound insulation curves with very low values in a single frequency band. Adaption term $C_{50\text{-}3150}$ represents the sound insulation of pink noise and $C_{tr,50\text{-}3150}$ represents the insulation of traffic noise. The index "50-3150" means that the adaption terms are calculated for the frequency range 50-3150 Hz which is the range used in this project (other ranges can also be used). (ISO 717-1:1996(E))

3 The Model

A rectangular plate surrounded by an infinite baffle is excited by a plane sound wave incident at an angle from the normal of the plate. The vibration induced by the incident wave causes radiation of sound from the plate. Diffuse field incident and radiated power is obtained by summing the contributions corresponding to all angles of incidence. Excitation and response is modelled in Comsol Multiphysics v. 4.1 while sound radiation calculations based on the Rayleigh integral are executed in Matlab 2009b.

The main assumptions and idealizations of the model are:

- fluid loading can be neglected
- only far field radiation is considered
- the wall is situated in an infinite baffle
- diffuse field excitation and radiation can be modelled by superposition of plane waves

The model is made using the Comsol plate interface which is "closer to the 2D plane stress condition than to the 3D solid" and does take transverse shearing into account (Comsol User's Guide).

Boundary conditions

The boundary conditions are thought of as a continuous distribution of springs acting on translational displacement and rotation about the edge axes as can be seen in figure 3.1.

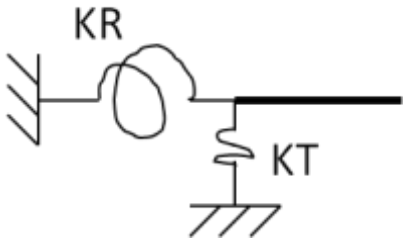

Figure 3.1 Boundary conditions defined as translational and rotational continuous springs.

In Comsol the boundary conditions are defined as edge loads with a force proportional to the transverse displacement and a moment proportional to the rotation. The constants of proportionality for the loads are equal and constant for all edges. Structural damping through complex modulus is used for both spring types as well as for the plate itself.

3.1 Excitation

It is assumed that the incident plane wave is totally reflected and the pressure doubled at the surface of the plate. The sound power inserted into the plate is thus assumed to be much less than the incident power. Since the relation between incident and radiating sound power is studied here, the amplitude of the exciting pressure is irrelevant and is therefore set to 1 Pa, i.e. symbolizing

an incident plane wave with free field pressure amplitude ½ Pa. The spatial distribution of pressure is determined by the angles of incidence and the frequency.

$$p_{ex}(x,y) = \exp\left[jk(\sin(\theta)\cos(\phi)x + \sin(\theta)\sin(\phi)y)\right] \quad (3.1)$$

where θ and ϕ are defined as in figure 2.2. θ is varied between 0 and 78°.

3.2 Sound Radiation

The Comsol data was exported as .txt-files containing the triangular element coordinates and the complex transversal velocity at the nodes. The Matlab code is presented in Appendix A. A rectangular grid was created in order to facilitate numerical operations and the velocity at the plate was interpolated from the nodal velocities. The real and imaginary parts of the nodal velocities were interpolated separately using the Matlab class `TriScatteredInterp` twice and adding the imaginary and real meshes to form a complex mesh. The default linear interpolation was used. The nodes in the grid were chosen so that there were 6 nodes per critical frequency bending wavelength below the critical frequency and 6 nodes per acoustic wavelength above the critical frequency, i.e. six nodes per wavelength were used for the smallest wavelength at each frequency.

The far field sound pressure at a point in the positive half-space is obtained from the Rayleigh integral as (Berry et al. 1990)

$$p(R,\theta,\varphi) = -\rho\omega^2 \frac{e^{-jkR}}{2\pi R}\eta(k_x,k_y) \quad (3.2)$$

where $\eta(k_x,k_y)$ is the wave number component of the displacement field over the plate (Berry et al. 1990).

$$\eta(k_x,k_y) = \frac{ab}{4}\int_{-1}^{1}\int_{-1}^{1}\eta(\alpha,\beta)\exp\left[j\left(\frac{a}{2}k_x\alpha + \frac{b}{2}k_y\beta\right)\right]d\alpha d\beta \quad (3.3)$$

a and b are the length and width of the plate respectively, α and β are dimensionless coordinates

$\alpha = 2x/a \qquad \beta = 2y/b$

Equation (3.3) is solved numerically by the approximating sum

$$\eta(k_x,k_y) = \frac{ab}{4}\sum_{n=1}^{N}\sum_{m=1}^{M}\eta(\alpha_n,\beta_m)\exp\left[j\left(\frac{a}{2}k_x\alpha_n + \frac{b}{2}k_y\beta_m\right)\right]w_n w_m \quad (3.4)$$

where (α_n,β_m) denotes a point at the plate and N and M are the number of points in the x- and y- direction respectively which must be odd numbers. The weights w_n and w_m are chosen according to Simpson's rule

$$w_{ends} = h/3, \qquad w_{even} = 4h/3,\ w_{odd} = 2h/3 \tag{3.5}$$

h is the uniform distance between evaluation points as is depicted in figure 3.2. Simpson's rule corresponds to fitting a piece-wise second order polynomial to the calculated node values.

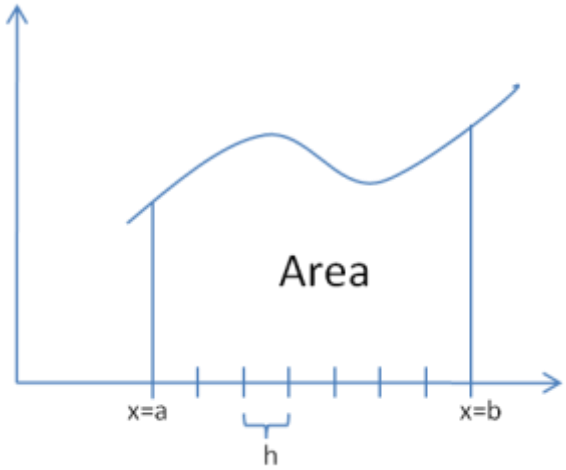

Figure 3.2 Area below curve.

The radiating power is given by integrating radial intensity over a hemisphere of infinite radius (Berry et al. 1990)

$$P = \frac{\rho\omega^4}{8c\pi^2}\int_0^{2\pi}\int_0^{\pi/2}\left|\eta(k_x, k_y)\right|^2 \sin\theta \, d\theta d\varphi \tag{3.6}$$

which is equivalent to integration of the wave number spectrum as described above. Since the wave numbers still depend on the angles φ and θ, equation (3.6) is approximated as a sum of the contributions to all discrete angles θ_q and φ_p.

$$P = \frac{\rho\omega^4}{8c\pi^2}\sum_{q=1}^{Q}\sum_{p=1}^{P}\eta(k_x, k_y)\sin(\theta_q)w_q w_p \tag{3.7}$$

Once again w are the weights of the integral approximation according to Simpson's rule, see equation (3.5).

3.3 Transmission loss

The incident sound power is the sound intensity on the surface of the plate multiplied by the surface area. The intensity is given (for this model) by the sound pressure multiplied by the velocity normal to the plate without the presence of the plate. For a plane wave incident at an angle θ_i from the normal, the power is given by

$$P_{inc}(\theta_i) = ab\frac{\left|\underline{p}\right|^2}{2\rho c}\cos(\theta_i) \tag{3.8}$$

where p is half the excitation pressure because of the assumed pressure doubling at the surface. By exciting the plate by a plane sound wave incident at angle θ_i the radiated sound power $P_{rad}(\theta_i)$ is obtained which is power radiated in all directions in the positive half-space. The transmission loss is given by the ratio of the sum of all radiated power to the sum of all incident power.

$$TL = \frac{\sum P_{inc}(\theta_i)}{\sum P_{rad}(\theta_i)} \tag{3.9}$$

The Matlab codes used to calculate the transmission coefficient and the averaged transmission loss are presented in Appendix C and Appendix B respectively

3.4 Analysis of boundary conditions

The boundary conditions are evaluated using non-dimensional stiffness related to the bending stiffness of the plates. Non-dimensional translational stiffness k_T and rotational stiffness k_R are given by

$$k_T = K_T h^3/D \quad k_R = K_R h/D \tag{3.10}$$

where the capital K_T and K_R are the actual translational and rotational stiffness respectively and h is the thickness of the plate. With damping the stiffness become

$$K_T = \frac{k_T D}{h^3}(1 + j\eta_T) \qquad K_R = \frac{k_R D}{h}(1 + j\eta_R) \tag{3.11}$$

4 Parameter study

When implementing the model there are a number of parameters that will affect the results. A parameter study is performed in order to investigate the possible errors caused by for example numerical integration. The main limitations caused by the implementation of the model are:

- the number of elements in the FE mesh
- the number of points for calculation of radiated sound power
- the number of incidence angles used to obtain "field incidence"
- the number of angles used for calculating radiated power
- the frequency resolution

The parameter study is only made for lightweight concrete walls and the results are then used also for the concrete wall and the gypsum board wall only increasing the finite element mesh fineness for the gypsum boards.

4.1 FE-Mesh

As a rule of thumb it is preferred to have 6 elements per bending wavelength in order to accurately derive natural frequencies (Fahy pp. 469-470). It is not obvious that this choice of mesh size also holds when modelling forced vibration since the pressure field of incident plane waves and the boundaries contribute to wave numbers (and wavelengths) differing from those of the free vibration. Moreover, wavelength of the incident plane waves also have to be correctly modelled and those wavelengths differ from the free bending wavelength. The FE mesh is triangular by default in Comsol. Predefined mesh sizes extra fine and extremely fine are compared in figure 4.1 considering the result on the space averaged square velocity on the plate. Extra fine and extremely fine give approximately 4 and 9 elements respectively per free bending wavelength at the highest frequency of interest.

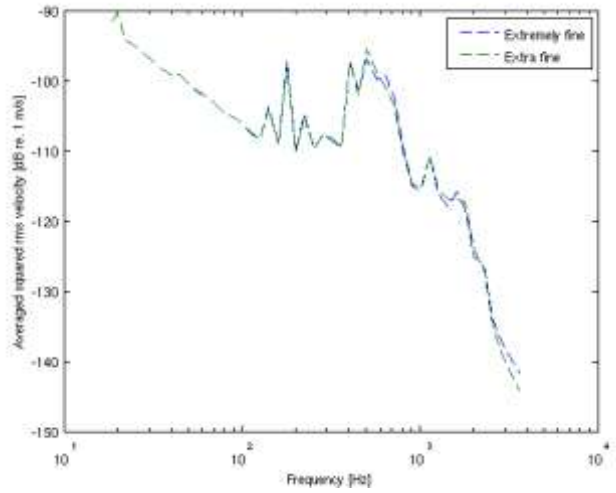

Figure 4.1 Space and time averaged velocity of a vibrating free lightweight concrete wall excited by a plane wave using two different element sizes.

Although the difference between the curves in figure 4.1 is small for frequencies below 3 kHz it is found by studying the radiation efficiency curves in figure 4.2 that the model probably is not valid above 1600 Hz. 1600 Hz is well above the critical frequency of the lightweight concrete wall where the logarithmic radiation efficiency is approximately 0 dB and independent of the type of excitation (Cremer et al. 2005).

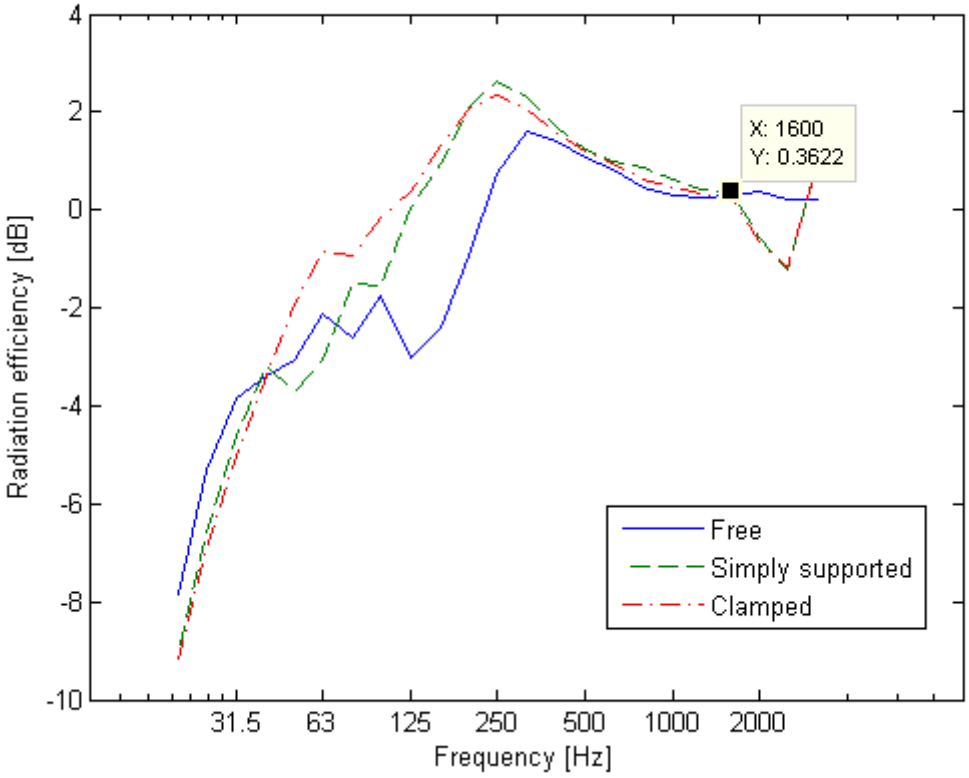

Figure 4.2 Radiation efficiency of a lightweight concrete wall for three different boundary conditions.

An *extra fine* mesh was chosen for the lightweight concrete wall, weighing computation time in favour of accurate calculations above 1600 Hz and the values of the transmission loss above this frequency was replaced by the values taken from equation (2.14). This modification was made so that the weighted sound reduction index could be calculated without using probably inaccurate transmission loss values. Even though the values from equation (2.14) may not be completely accurate, the values are independent of the boundary conditions which enables comparison of the sound insulation at lower frequencies without taking errors at high frequencies into account. The modification step is also motivated by the fact that the original transmission loss curves seem to converge to these theoretical values at high frequencies. The extra fine mesh is used for the gypsum board wall giving approximately two elements per bending wavelength at the highest frequencies. The accuracy at high frequencies for all wall types will therefore be limited.

4.2 Number of radiation angles

The number of angles to use for the numerical approximation of the integral in equation (3.6) is chosen by a parameter study of the total radiated power. θ is assumed to be more important since the number of angles determines the number of coincidence frequencies. Thus the number of angles is equal for both coordinates although θ ranges from 0 to π/2 radians and φ from 0 to 2π. The radiated power using 31, 45 and 61 angles is compared in figure 4.3 and it is clear that the difference is negligible, thus 45 angles were chosen. The comparison was done for a free lightweight concrete wall.

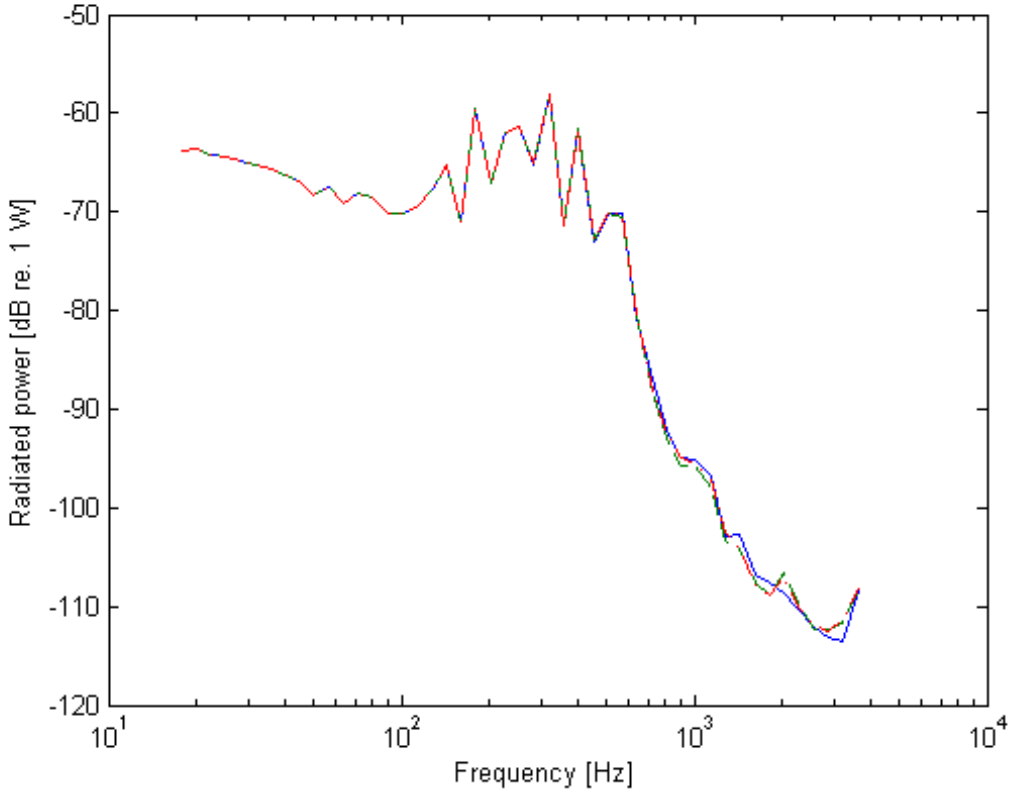

Figure 4.3 Radiated power from a vibrating concrete wall. (-) 31 angles, (--) 45 angles and (-.) 61 angles.

4.3 Number of excitation angles

It is assumed that the colatitude coordinate θ of the incident wave is of great importance because of the trace wavelengths (with corresponding coincidence frequencies) and that the longitude coordinate φ is less important. 2, 8, 16, 32 and 48 colatitude coordinates are used in a parameter study and the corresponding radiated sound power is compared. The curves in figure 4.4 represent the radiated sound power from a free lightweight concrete wall corresponding to the number of excitation angles. The curves for 32 and 48 angles coincide and consequently 32 angles are chosen to represent field

incidence. Because of the long computation time per angle of incidence, the influence of the number of longitude coordinates was not investigated.

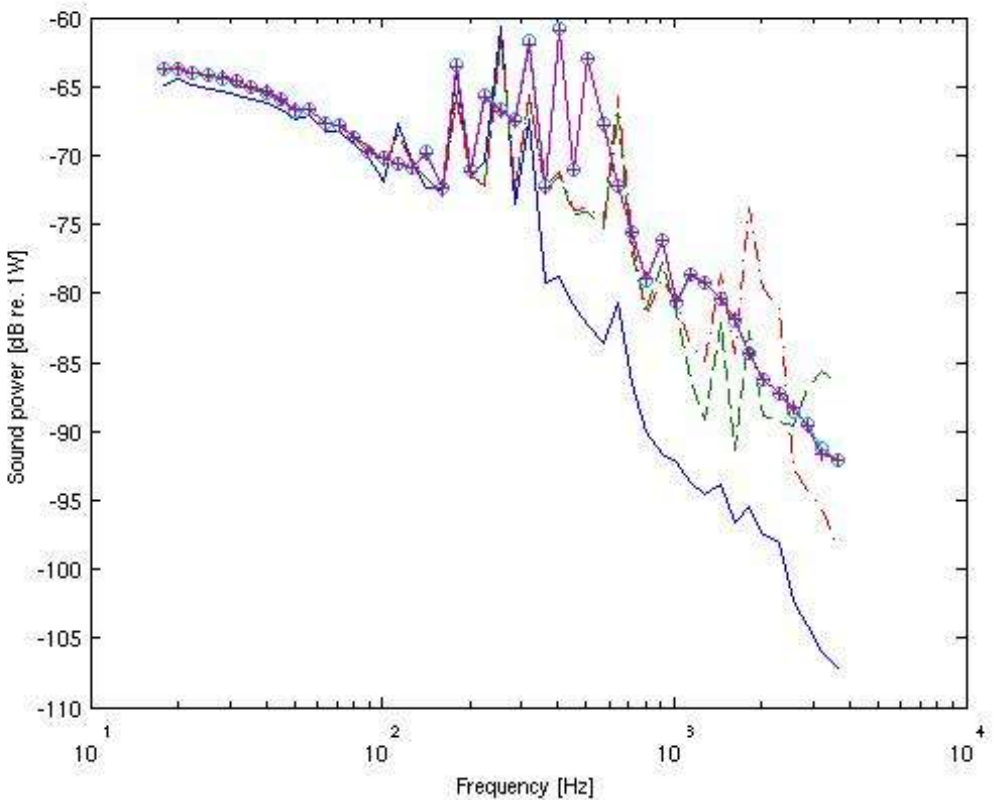

Figure 4.4 Radiated sound power for different numbers of incidence angles. (-), 2 angles, (--), 8 angles, (-.) 24 angles, (+), 32 angles and (o), 48 angles.

Range of the boundary condition values

In order to confine the boundary condition parameter study, two extreme values for each type of non-dimensional stiffness is found by using the idealized cases free, simply supported and clamped edges as references. These extreme values are listed in table 4.1 and constitute the limits of the boundary condition parameter study.

Table 4.1Limits of the non-dimensional boundary conditions for the three wall types.

Lightweight concrete	Min	Max
$\log_{10}(k_T)$	-3	3
$\log_{10}(k_R)$	-3	3
Gypsum boards		
$\log_{10}(k_T)$	-5	3
$\log_{10}(k_R)$	-5	3
Concrete		
$\log_{10}(k_T)$	-4	2
$\log_{10}(k_R)$	-4	2

The transmission loss curves for free, simply supported and clamped lightweight concrete walls are presented together with their finite counterparts in figure 4.5. By finite counterparts is meant the finite extremes of the boundary conditions which constitute the outer limits of the parameter study. Continuous lines for the idealized cases and dashed lines for their counterparts. The differences are hardly noticeable except for rather large deviations between the free and the almost free walls above 100 Hz which implies that the lowest limits of stiffness are not low enough.

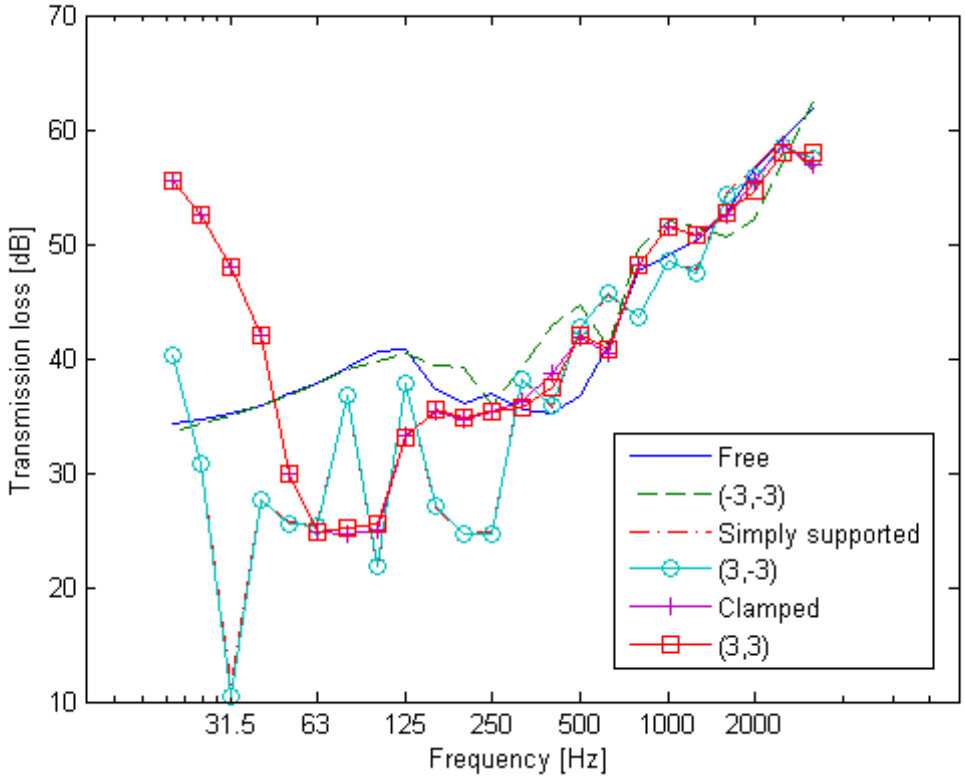

Figure 4.5 Transmission loss curves for finite, non-zero boundary conditions and the idealized cases.

4.4 Validation

Since no measurements are made the model is compared to theoretical curves and measured transmission loss of a wall with unknown boundary conditions. In figure 4.6 the transmission loss of a free lightweight concrete wall is presented along with a theoretical curve based on equations (2.12) and (2.14) and measured transmission loss of a similar wall (Long, M. 2003) with same thickness and material properties as the modelled light concrete wall.

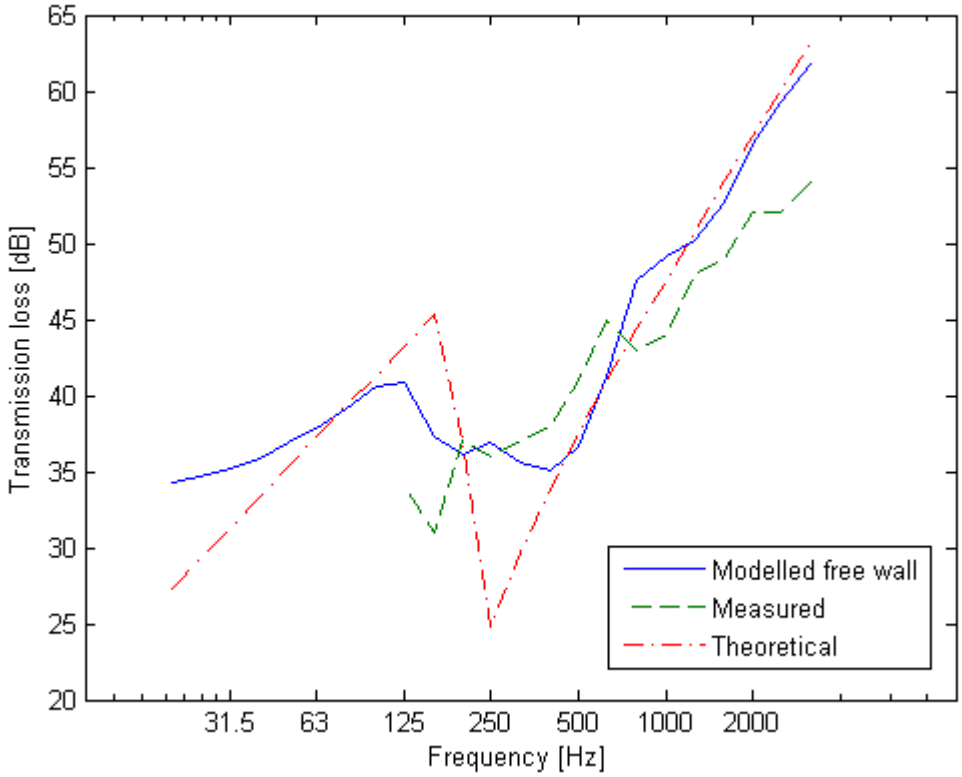

Figure 4.6 Transmission loss curves for modelled and measured wall as well as infinite panel theory.

The theoretical curve is based on infinite wall theory which is why the transmission loss is lower than the modelled wall at very low frequencies and the dip at the critical frequency is excessive. At high frequencies the modelled and theoretical curves agree very well but the measured transmission loss is considerably lower.

4.5 Frequency resolution

Calculations were made for the centre frequencies and band limits of 1/3-octave bands. This rather coarse frequency resolution was chosen in order to restrict the calculation time. The matter is discussed in chapter 6.

5 Results

Selected transmission loss and radiation efficiency curves are presented here together with corresponding weighted sound reduction indices and adaption terms $C_{50\text{-}3150}$ and $C_{tr,50\text{-}3150}$. The transmission loss curves are presented in their original form while the weighted sound reduction indices for the concrete and lightweight concrete walls are calculated from the modified transmission loss at high frequencies described in chapter 4.

5.1 Lightweight concrete wall

The material properties of the 4.2x2.6x0.2 m3 lightweight concrete wall were chosen as follows: density $\rho = 1300$ kg/m3, Young's modulus $E = 3.8$ GPa, Poisson's ratio $\mu = 0.3$ [-] and loss factor $\eta = 0.015$ [-]. The loss factor of the boundary springs was 0.05 for both deflection and rotation. The critical frequency is 180 Hz.

The non-dimensional stiffness coefficients are organized in a diagram in figure 5.1 where one point represents one combination of boundary conditions. The symbols at the corners represent (counter clockwise starting from lower left corner) free, simply supported and clamped edges respectively.

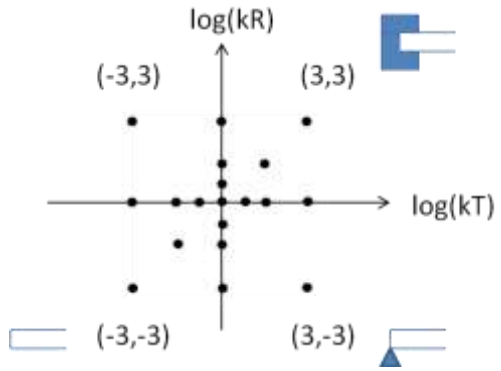

Figure 5.1 Different boundary conditions organized in a diagram.

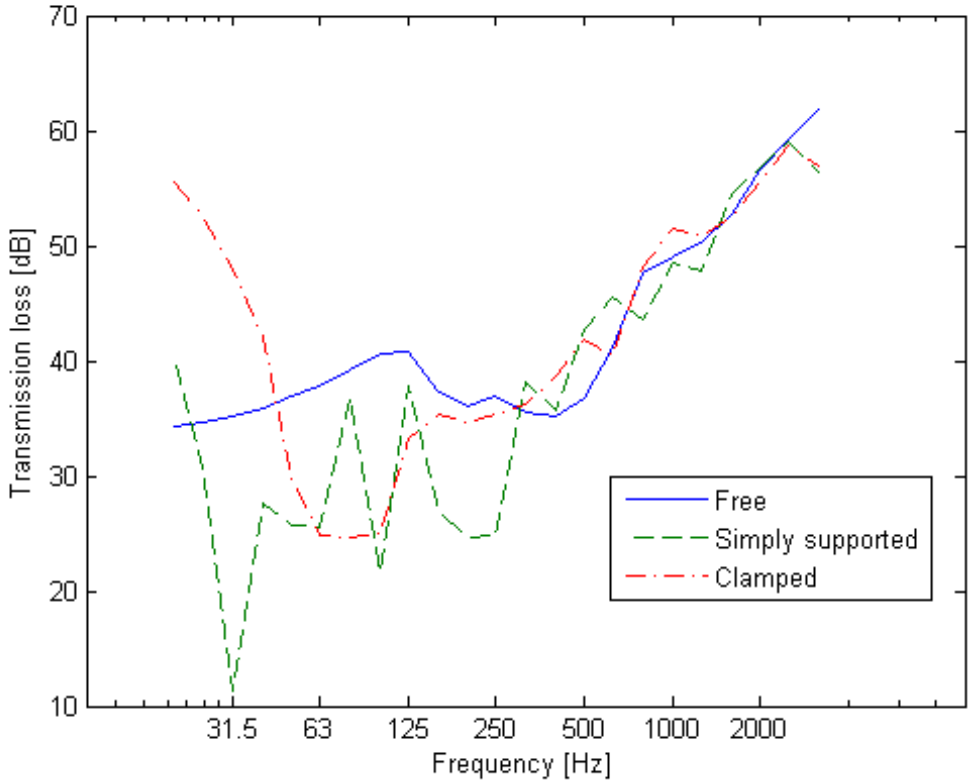

Figure 5.2 Transmission loss curves corresponding to different boundary conditions of a lightweight concrete wall.

Table 5.1 Weighted sound reduction index and adaption terms corresponding to different boundary conditions of a lightweight concrete wall.

	$R_w(C_{50\text{-}3150}; C_{tr,50\text{-}3150})$
Free	45(-1;-4)
Simply supported	42(-3;-7)
Clamped	46(-2;-7)

The first resonances occur at rather high frequencies and the critical frequency is quite low for the lightweight concrete wall. The transmission loss curves in figure 5.2 show that the transmission is very much influenced by the resonances below the critical frequency. The difference between the curves is large below 250 Hz while the difference is fairly small at high frequencies. The difference in weighted reduction index and adaption terms for different boundary conditions is substantial as is seen in table 5.1.

Figure 5.3 shows the transmission loss curves for different boundary conditions, all having the dimensionless rotational stiffness exponential $\log(k_R)$ equal to zero and different dimensionless translational stiffness

exponential log(k_T) varying from -3 to 3, i.e. moving horizontally along the log(k_T) axis in the diagram in figure 5.1.

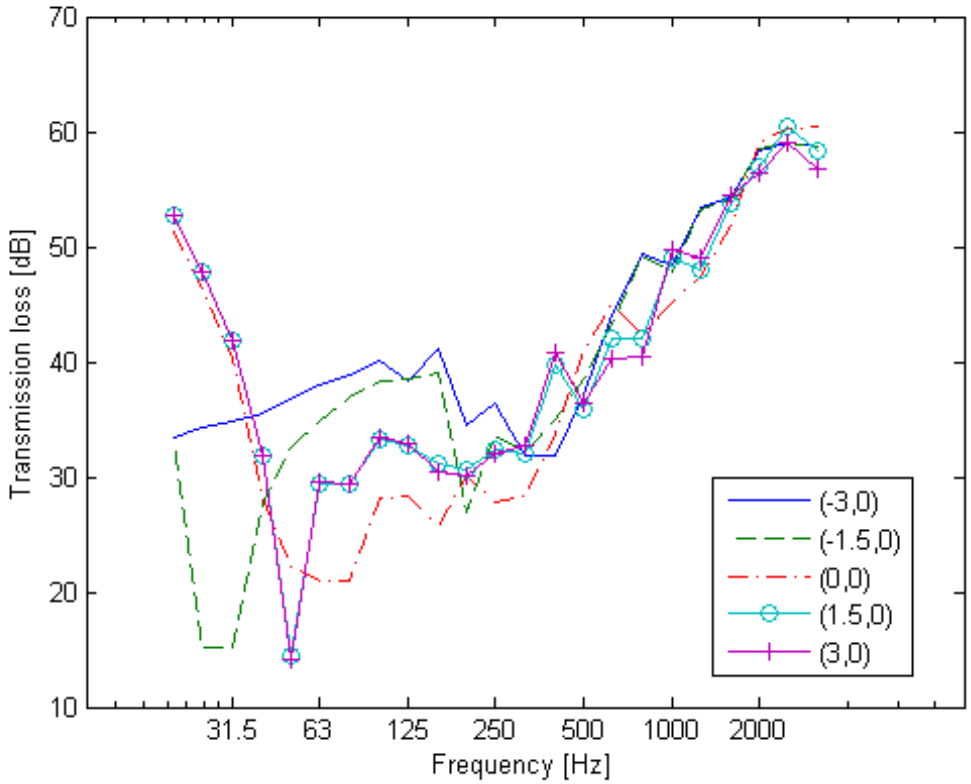

Figure 5.3 Transmission loss curves corresponding to different boundary conditions of a lightweight concrete wall.

Table 5.2 Weighted sound reduction index and adaption terms corresponding to different boundary conditions of a lightweight concrete wall.

(log(kT),log(kR))	$R_w(C_{50\text{-}3150}; C_{tr,50\text{-}3150})$
(-3,0)	44(-2;-4)
(-1.5,0)	43(-1;-4)
(0,0)	41(-2;-7)
(1.5,0)	43(-1;-7)
(3,0)	43(-1;-7)

Considering the single number quantities given in table 5.2 it is apparent that low translational stiffness gives the best low frequency sound insulation. Figure 5.4 shows the transmission loss when log(k_T) is fixed to zero and log(k_R) is varied from -3 to 3, i.e. moving vertically along the log(k_R) axis in the diagram in figure 5.1.

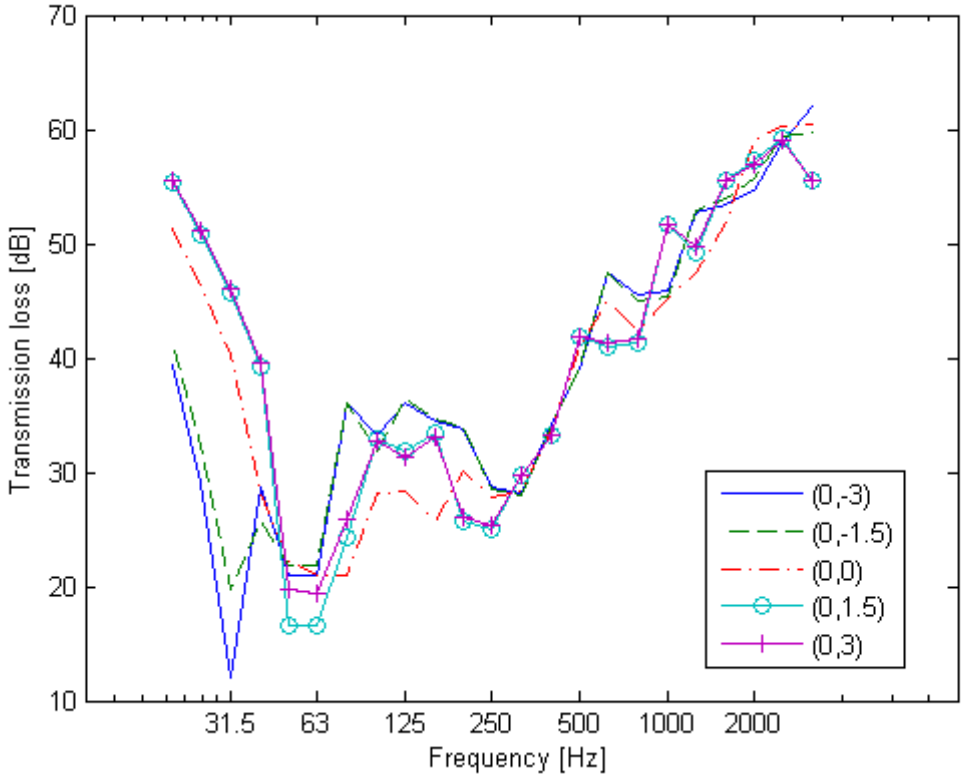

Figure 5.4 Transmission loss curves corresponding to different boundary conditions of a lightweight concrete wall.

Table 5.3 Weighted sound reduction index and adaption terms corresponding to different boundary conditions of a lightweight concrete wall.

($\log(k_T)$,$\log(k_R)$)	$R_w(C_{50\text{-}3150}; C_{tr,50\text{-}3150})$
(0,-3)	43(-2;-7)
(0,-1.5)	43(-2;-7)
(0,0)	41(-2;-7)
(0,1.5)	41(-2;-8)
(0,3)	41(-2;-7)

An increase of rotational stiffness clearly lowers the sound insulation according to table 5.3.

Figure 5.5 shows the transmission loss when varying $\log(k_T)$ and $\log(k_R)$ from -3 to 3 in steps of 1.5 simultaneously, i.e. moving diagonally in the diagram in figure 5.1 from free to clamped.

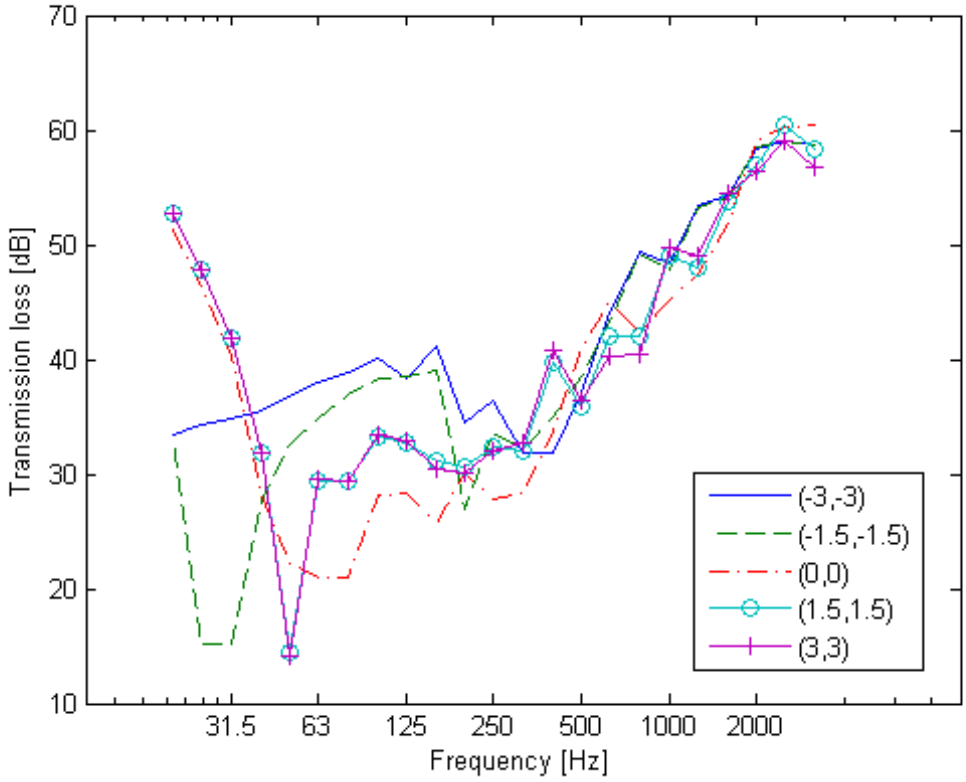

Figure 5.5 Transmission loss curves corresponding to different boundary conditions of a lightweight concrete wall.

The weighted sound reduction index has its lowest value when the wall has boundary values somewhere between free and clamped. The sound insulation is improved when the boundary conditions approach those of a clamped wall but the low frequency transmission loss is still much lower than the for free wall. Note that the almost free wall in table 5.4 has much higher sound reduction index compared to the completely free wall in table 5.1 (48 dB and 45 dB respectively).

Table 5.4 Weighted sound reduction index and adaption terms corresponding to different boundary conditions of a lightweight concrete wall.

$(\log(k_T),\log(k_R))$	$R_w(C_{50\text{-}3150}; C_{tr,50\text{-}3150})$
(-3,-3)	48(-1;-4)
(-1.5,-1.5)	45(-3;-7)
(0,0)	41(-2;-7)
(1.5,1.5)	46(-1;-7)
(3,3)	46(-2;-7)

5.2 Gypsum board wall

The gypsum board wall is composed of two identical gypsum boards positioned together with no distance in between but only attached to one another at the common boundaries. According to experience, composite structures of two gypsum boards keep the critical frequency of the single board (Thorsson, P. 2011). Since the total mass must be doubled this means that the bending stiffness must be doubled too and not multiplied by 2^3 as would be the case for a homogenous structure with doubled thickness. Hence, the thickness of one board is used while the mass density and modulus of elasticity are doubled. The boundaries considered here are the attachments of gypsum board edges to joists which is why the dimensions of the gypsum board wall is chosen as standard board dimensions instead of the dimensions of a complete wall construction. The gypsum wall (composite structure) has dimensions 1.2x2.6x0.0125 m3, density $\rho = 2 * 720$ kg/m3, Young's modulus $E = 2 * 2$ GPa, Poisson's ratio $\mu = 0.3$ [-] and loss factor $\eta = 0.006$ [-]. It is assumed that the losses at boundaries are high, hence the boundary spring loss factors are 0.10 [-]. The critical frequency is at 3 kHz.

The element size does not fulfil the condition of 6 elements per wavelength at the highest frequencies for the gypsum board wall but the results show at least an expected pattern which is why the transmission loss curves are used in their original form and no values are replaced by theoretical values. The transmission loss curves for the free, simply supported and clamped gypsum board walls are presented in figure 5.6 together with the theoretical curve taken from equations (2.12) and (2.13).

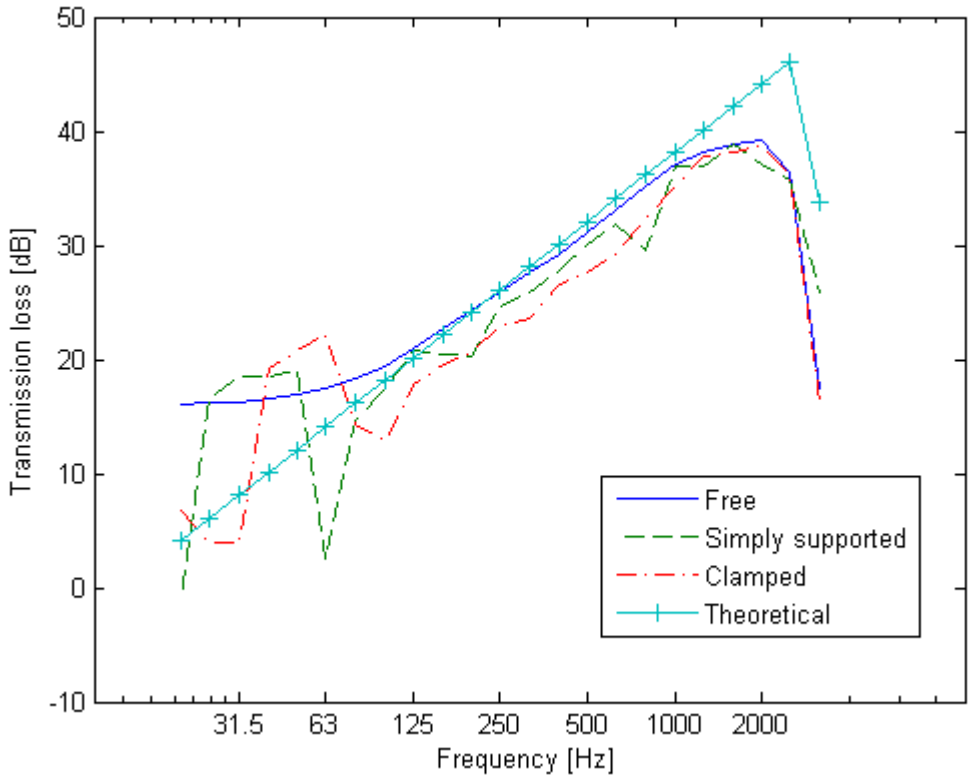

Figure 5.6 Transmission loss curves corresponding to different boundary conditions of a gypsum board wall.

The transmission loss of the free wall is approximately 3 dB higher than the clamped and simply supported walls. The difference between the simply supported wall and the clamped wall is negligible except for a transmission loss dip at 63 Hz for the simply supported wall which is also seen in the very low $C_{tr,50\text{-}3150}$ term in table 5.5.

Table 5.5 Weighted sound reduction index and adaption terms corresponding to different boundary conditions of a gypsum board wall.

	$R_w(C_{50\text{-}3150}; C_{tr,50\text{-}3150})$
Free	33(-7;-5)
Simply supported	32(-2;-9)
Clamped	30(-6,-5)

The radiation efficiency corresponding to the boundary condition extremes are presented in figure 5.7. Note that the free wall radiation efficiency approaches 0 dB far below the critical frequency!

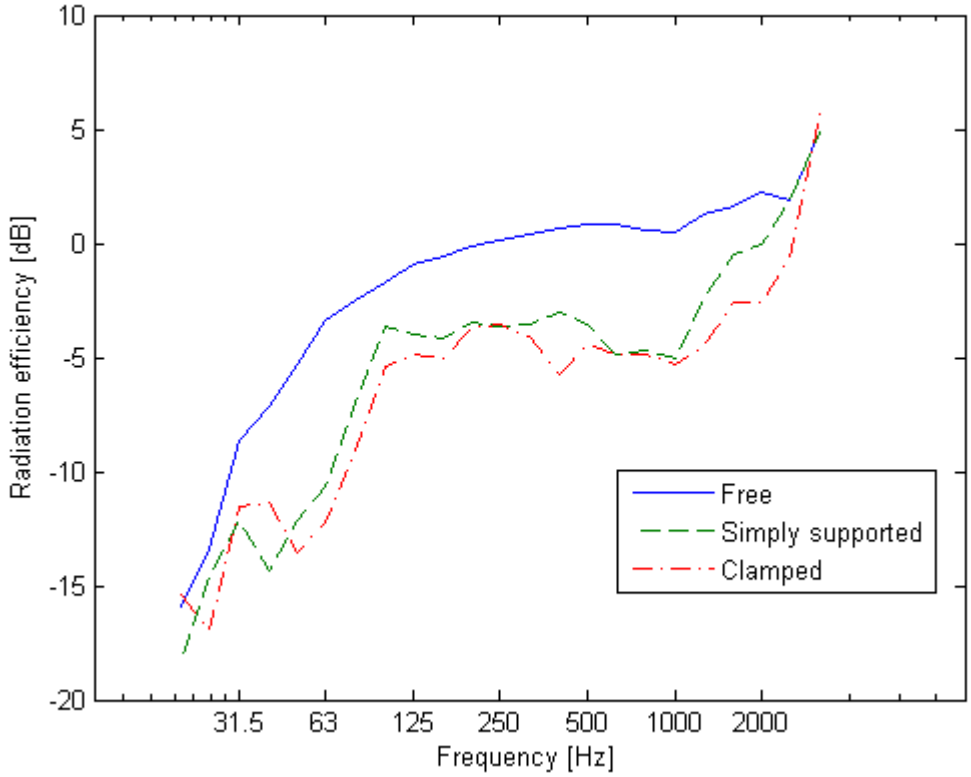

Figure 5.7 Radiation efficiency curves corresponding to different boundary conditions of a gypsum board wall.

Figure 5.8 shows the transmission loss curves corresponding to the boundary conditions when increasing both translational and rotational stiffness simultaneously from almost free to almost clamped (compare with figure 5.5) and the corresponding weighted reduction indices and adaption terms are given in table 5.6.

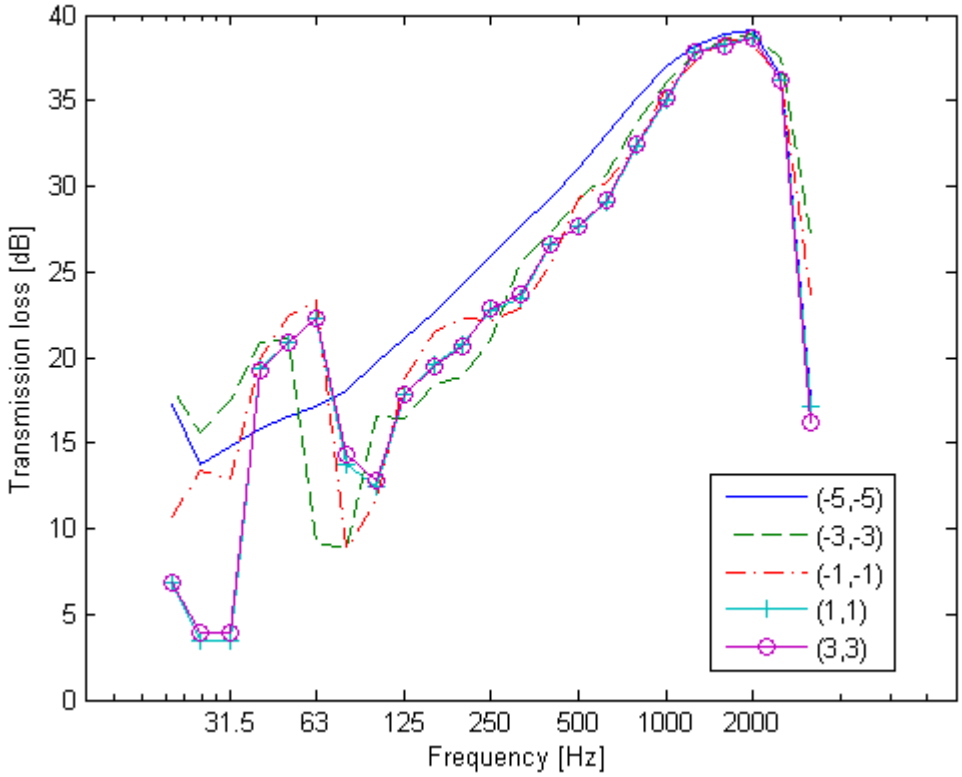

Figure 5.8 Transmission loss curves corresponding to different boundary conditions of a gypsum board wall.

Table 5.6 Weighted sound reduction index and adaption terms corresponding to different boundary conditions of a gypsum board wall.

	$R_w(C_{50\text{-}3150}; C_{tr,50\text{-}3150})$
(-5,-5)	33(-7;-5)
(-3,-3)	32(-2;-7)
(-1,-1)	31(-2;-6)
(1,1)	30(-5;-5)
(3,3)	30(-6;-5)

Compared to the lightweight concrete wall the differences in weighted sound reduction index are not as big for the gypsum board wall. The first few resonances of the wall are quite low in frequency and do not have a major influence on the sound transmission at the frequency span considered for the single valued quantities.

5.3 Concrete

The concrete wall has the same dimensions as the lightweight concrete wall except for the thickness which is 0.16 m. The critical frequency is 115 Hz. In figure 5.9 the transmission loss curves for the free, simply supported and clamped concrete walls are presented together with the theoretical curve given by equations (2-12), (2.13) and (2.14).

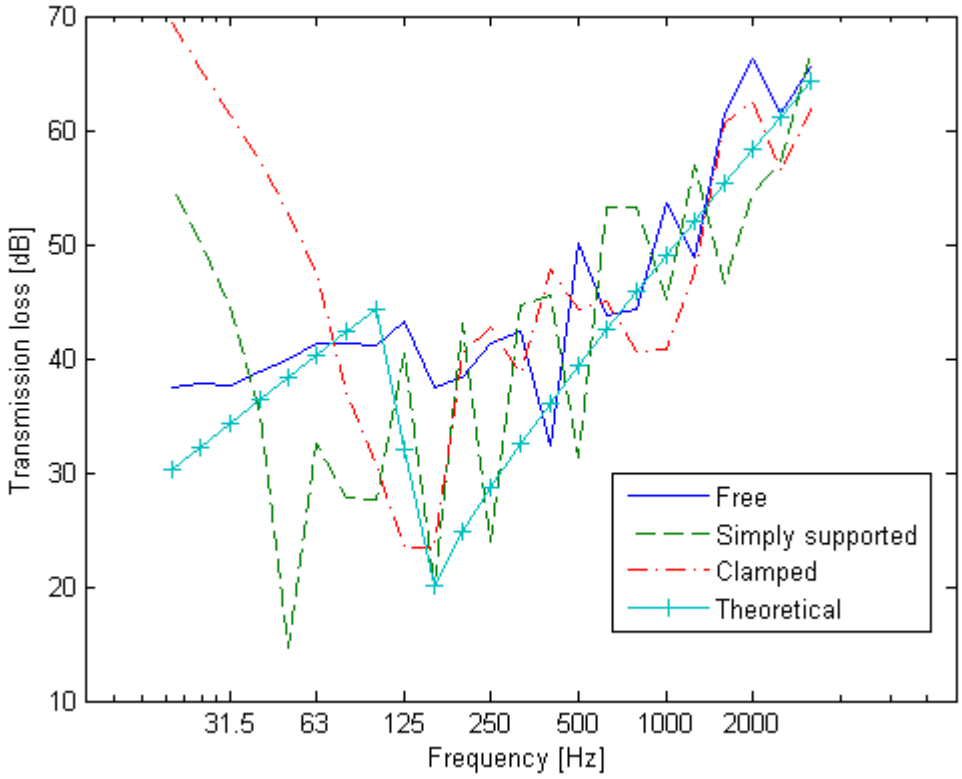

Figure 5.9 Transmission loss curves corresponding to different boundary conditions of a concrete wall.

As is seen in table 5.7 the sound insulation is very much influenced by the boundary conditions and the free wall has a 6 dB higher weighted sound reduction index compared to the simply supported wall.

Table 5.7 Weighted sound reduction index and adaption terms corresponding to different boundary conditions of a concrete wall.

	$R_w(C_{50\text{-}3150}; C_{tr,50\text{-}3150})$
Free	48(-3;-5)
Simply supported	42(-4;-9)
Clamped	44(-2,-6)

The radiation efficiency corresponding to free, simply supported and clamped edges are given in figure 5.10.

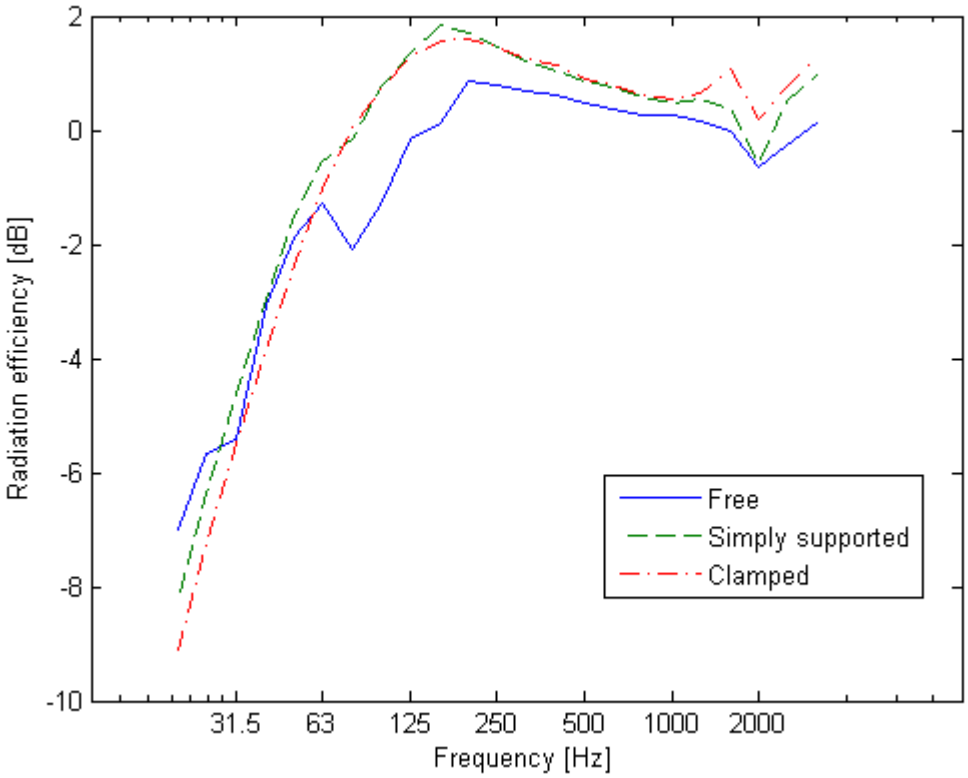

Figure 5.10 Radiation efficiency curves corresponding to different boundary conditions of a concrete wall.

The behaviour of the concrete wall is very similar to the lightweight concrete wall since they both have high first resonance frequencies and low critical frequency. The transmission loss curves in figures 5.9 and 5.11 show very resonant behaviour even far above the critical frequency.

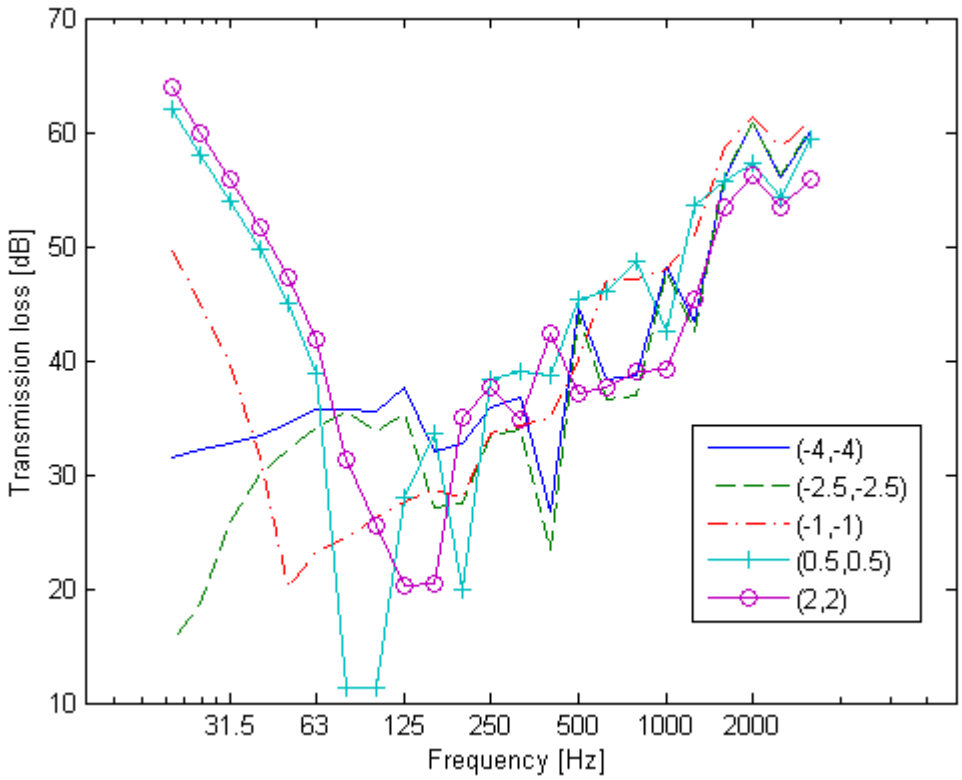

Figure 5.11 Transmission loss curves corresponding to different boundary conditions of a concrete wall.

In figure 5.11 the transmission loss curves corresponding to five different boundary conditions are plotted. As is seen in table 5.8, the weighted sound reduction indices do not differ as much as for the lightweight concrete wall. There is a very dominant dip in the transmission loss at about 100 Hz for the dimensionless stiffness coefficients (0.5, 0.5) which is also seen in the $C_{tr,50\text{-}3150}$ term in table 5.8. As opposed to the concrete wall the highest weighted sound reduction index is found for the dimensionless boundary conditions (-1,-1) which is in between free and clamped.

Table 5.8 Weighted sound reduction index and adaption terms corresponding to different boundary conditions of a concrete wall.

(log(kT),log(kR))	$R_w(C_{50\text{-}3150}; C_{tr,50\text{-}3150})$
(-4,-4)	48(-3;-5)
(-2.5,-2.5)	45(-3;-6)
(-1,-1)	49(-2;-7)
(0.5,0.5)	48(-6;-15)
(2,2)	46(-2;-6)

6 Discussion

The results hold only for walls of the studied dimensions and material properties and are not strictly applicable for general constructions. The dimensions of the lightweight concrete and concrete walls are however chosen so that they agree fairly well with standard walls separating rooms in residential buildings. The dimensions of the gypsum board construction are chosen as a standard board size. Since gypsum boards are typically attached to joists separated by a distance equal to the size of the boards it is reasonable to define the boundaries for each attachment and therefore the dimensions of the construction are adequate for general constructions.

6.1 The model

Limitations of the theoretical model are listed in chapter 3 and possible sources of error due to the implementation of the model are listed in chapter 4. These factors concerning the end result are discussed below.

6.1.1 Fluid loading

Only partitions having transmission loss above 20 dB are considered here which means that the incident sound power is more than a factor 100 greater than the radiated power. Since the radiated power is the real part of the fluid loading it can be argued that this loading is negligible compared to the in vacuo impedance of the partition. Considering a normally incident plane wave through an unbounded partition the fluid impedance equals twice the specific acoustic impedance of air and can easily be compared to the mass impedance of the partition. For oblique incidence and bending the analysis of wave impedances is more complex. The mass-like loading below the critical frequency and the resistive loading above the critical frequency both approach infinity when moving towards the critical frequency from their respective direction. However, experience shows that such phenomena do not occur in practice which can also be concluded theoretically by considering finite plates.

6.1.2 Far field

The far-field model was used for simplicity and because it seems to be a generally accepted simplification used in many models, e.g. Berry et al. (1990). However, equation (2.7) shows that the near-field waves approach infinity in distance from the plate when approaching the critical frequency which means that they are definitely not negligible. On the other hand this argument is based on the same simplifications as the infinite fluid loading discussion above and can therefore not reflect the radiation from a finite plate. However, the sound transmission through a partition does have a peak at the critical frequency in general because of the increase of resistive fluid loading and it is therefore reasonable to believe that also the reactive fluid loading is high around the critical frequency.

6.1.3 Infinite baffle

The infinite baffle is of course not a model representing a condition occurring in practice, especially when it comes to diffuse fields where rooms must be present. However, the aim of this study was to isolate the effects of boundary conditions and it was therefore a reasonable approach avoiding effects due to room shape and other parameters. Moreover, in a laboratory the test specimen is often situated in a so called test frame when sound insulation is measured and the specimen is therefore surrounded by a baffle if not an infinite one.

6.1.4 Field incidence excitation

By summing up the incident sound power it is assumed that the incident waves are uncorrelated which is the case also for a real diffuse field where angles of incidence and phase are totally random. The same argument holds for the radiated sound power which should also be uncorrelated and the diffuse field should therefore be modelled correctly. On the other hand it is obvious that a real diffuse field cannot be modelled omitting variation of the longitude coordinate ϕ. To what extent this omission is influencing the end result is not investigated which leads to a lack of reliability of the model. However, only the colatitude coordinate θ influences the trace wavelength and it is argued that the longitude coordinate only influence to what extent different modes are excited which should have a minor effect on the transmission loss, at least above the first resonances of the wall where the modal density is rather high and resonances considerably damped. The chosen number of angles θ seems to be sufficient according to the parameter study since increasing the number of angles above 32 did not have any effect on the radiation.

6.1.5 Finite element size

It may seem strange that in figure 4.1, the sound radiation is to such a small extent influenced by the mesh size even though the finer mesh size basically should lead to correct results and the coarser lead to incorrect results at the highest frequencies. This is probably only a coincidence and the coarser mesh only happened to work very well for the free wall. As seen in figure 4.2, the radiation efficiency of the free wall behaves exactly as expected while the radiation efficiency of the simply supported and clamped walls is obviously incorrect at frequencies where the element size is comparable to the wavelength of the exciting wave.

Considering free bending waves the extremely fine mesh should hold as high up in frequency for the gypsum board wall as the extra fine mesh does for the concrete and the lightweight concrete walls. However, the extremely fine mesh enables a more satisfying model of the excitation field which can be the reason why both transmission loss and radiation efficiency looks more as expected for the complete frequency span of interest.

6.1.6 Grid size for sound radiation

The decision to use the acoustic wavelength to dominate the size of the plate grid for the calculation of the radiated power did not come from any theoretical analysis. The wave number analysis is based on the vibration of the plate and no acoustic wave is really modelled, thus only the vibration pattern must be correctly reproduced. Nevertheless it was found that a decreasing the grid size so that there was 6 points per acoustic wavelength did make a slight difference on the radiated power which may be due to the fact that the vibration field on the wall contains wave numbers differing from the free bending wave number.

6.1.7 Number of angles for radiation

By looking at figure 4.3 it is clear that the reliability of the model is not at all affected by the number of angles used for calculating the radiated power.

Frequency resolution

The modal density of a plate is independent of frequency. Since the calculations are made for the band limits and centre frequencies of 1/3-octave bands the number of calculations per mode is low at high frequencies. The transmission loss curves are therefore not smoothened out appropriately which makes the evaluation at high frequencies complicated and probably less relevant.

6.2 Results

The interpretations of the results are made assuming that the model is completely reliable concerning representation of the idealized physical circumstances it is based on.

6.2.1 Lightweight concrete and concrete walls

The transmission loss of the lightweight concrete and concrete walls basically shows the same dependence upon boundary conditions. Both wall types have rather high first resonance frequencies and fairly low critical frequencies which is why the calculated transmission loss does not agree well with infinite panel theory. The walls seem to have low modal density even above the critical frequency and especially the concrete wall is lightly damped which is probably why the transmission seems to be dependent on relatively few structural modes. Below the critical frequency it is very easy to see how the transmission loss depends on how the first resonance frequencies are shifted but at higher frequencies the dependence seem to be more random and conclusions are more difficult to draw. Comparing the results from the model to measured transmission loss curves which are smoother there is reason to believe that the damping of the walls is not sufficient. Another reason may be the low frequency resolution which does not enable accurate averaging of sound transmission over the third octave bands. Already at 500 Hz there is less than one 1/6- octave band per resonance. Theoretically the transmission loss should be governed by coincidence effects above the critical frequency

but the dips in the transmission loss curves must be caused by structural resonances since dips caused by coincidence would occur at the same frequencies for all boundary conditions.

It is tempting to draw the conclusion that the sound transmission is dominated by the resonant modes and not forced vibration but comparing the radiation efficiency with theoretical values based on resonant vibration only (typically less than -10 dB below the critical frequency) it is much higher below the critical frequency implying that the forced transmission is also significant.

The fact that the critical frequency seems to be higher than the theoretical one is probably because the bending near field at the boundaries are comparable to the dimensions of the wall. The vibration pattern affected by forced bending and bending near fields may not match the acoustic field perfectly right at the theoretical critical frequency.

The lightweight concrete wall has its best sound insulation when the edges are free. Also by comparing the finite, non-zero boundary conditions (see tables 5.2, 5.3 and 5.4) it is found that the sound insulation is improved by making the edges less restrained. Approaching clamped conditions the sound insulation is also satisfying, except at low frequencies.

The concrete wall on the other hand does not show an equally clear dependence on boundary conditions. By studying the results given in table 5.8 it is seen that the sound insulation is very much dependent on the boundary conditions but it is not as easy to find certain boundary conditions for which the sound insulation is optimal. Small changes of boundary stiffness give rather large differences in weighted sound reduction index.

6.2.2 Gypsum board wall

The transmission loss of the free gypsum board wall agree very well with mass law and the radiation efficiency approaches unity far below the critical frequency which indicates that the transmission is forced. The transmission loss of the restrained walls is clearly dominated by single resonances up to about 100 Hz. Above this low frequency range the difference between the various edge conditions is rather small. Only the free wall has a higher transmission loss for all frequencies above 100 Hz.

6.2.3 General considerations

Since the difference in transmission loss is much bigger than the difference in radiation efficiency for different edge conditions it is concluded that the wave mobility and the resonances are much more important than the resulting shape of the vibration. The gypsum board wall clearly indicates this since the free wall has substantially higher radiation efficiency but still has a higher transmission loss over the whole frequency range compared to the other edge

conditions. The excitation of vibration modes seems to be negligible for free walls and the transmission is strictly forced. For all other edge conditions the resonant modes are much easier excited which adds more vibration energy and radiation. The results are in agreement with the results obtained by Sewell (1970) where another method is used for calculating the diffuse field transmission loss of a single panel.

At very low frequencies the free walls have higher transmission loss than predicted by mass law which is interpreted as a consequence of the wall moving in agreement with mass law but the finite wall radiates much less efficiently when the acoustic wavelength is comparable to the wall dimensions.

According to Smith (1964), subcritical radiation efficiency of a clamped wall is twice as high as for a simply supported wall above the first mode. In the short frequency range between first resonance and critical frequency for lightweight concrete wall, the radiation efficiency is higher for the clamped wall than for the simply supported in accordance with this theory. For the gypsum board wall the relationship is the opposite and does therefore not agree with the mentioned theory. One possible reason for this behaviour is that the forced vibration radiation in some way is attenuated by the clamped edges (Smith studied modal radiation only). Concerning the concrete wall this frequency range is too short for any such behaviour to appear.

7 Conclusions

According to this study the sound insulation seems to depend on the amount of vibration energy that is induced in the wall rather than how well the wall radiates sound. There does not seem to be a clear relation between radiation efficiency and the induced vibration energy. Considering the concrete, lightweight concrete and gypsum board walls studied in this project, the boundary conditions have a significant influence on the transmission loss.

Free edges give the best sound insulation considering the whole frequency range. Resonant transmission seems to be negligible for free walls. The stiffer the boundaries, the lower the transmission loss at low frequencies because the first resonances of the wall are shifted upward in frequency.

Above the critical frequency the dependence on boundary conditions seems quite random and it is therefore difficult to draw any general conclusions. A higher frequency resolution would probably make the transmission loss curves smoother and would make the comparison of different curves more relevant. Considering the gypsum board wall for which the whole studied frequency range lies below the critical frequency it is safe to say that the sound insulation is optimized by making the boundaries less restrained.

Future perspective

The model needs to be improved. It is very time consuming and imprecise. The purpose of this project was to study the influence of boundary conditions on the sound insulation over the major part of the frequency range considered in the field of building acoustics but maybe it would be a better idea to limit the frequency range in favour of the number of frequencies in order to attain more accurate results. A less time consuming way of modelling diffuse field excitation would also be of great interest.

Finally it is of utmost importance that the results from any model are compared to experimental results. Assessing real life boundary conditions is the first problem to solve before laboratory measurements can be performed.

8 References

Berry, A & Guyander, J-L & Nicolas, J (1990) *A general formulation for the sound radiation from rectangular, baffled plates with arbitrary boundary conditions*. Journal of the Acoustical Society of America 88

Chiello, O. & Sgard, F.C. & Atalla, N. (2003). *On the use of a component mode synthesis technique to investigate the effects of elastic boundary conditions on the transmission loss of baffled plates*. Computers and Structures 81 pp. 2645-2658.

Comsol Multiphysics v. 4.1 User's Guide

Cremer, L., Heckl, M. & Petersson, B.A.T. (2005). *Structure-borne Sound, third edition*. Springer-Verlag.

Fahy, F. & Gardonio, P. (2007). *Sound and Structural Vibration, Second Edition*. Academic Press.

Forssén, J. (2010). *Building Acoustics and Community Noise, Lecture Notes*. Chalmers University of Technology.

Gyproc Handbook 7 (2007). Erlanders Berlings. Malmö

ISO 717-1:1996(E) *Acoustics – Ratings of sound insulation in buildings and of building elements.*

Kihlman, T. (1970). *Sound transmission in building structures of concrete*. Journal of Sound and Vibration vol. 11(4) pp. 435-445.

Kihlman, T. & Nilsson, A. C. (1972). *The effects of some laboratory designs and mounting conditions on reduction index measurements*. Journal of Sound and Vibration 24 (3) pp. 349-364.

Kropp, W. (2007). *Lecture notes, Technical acoustics*. Chalmers University of Technology.

Long, M. (2006). *Architectural Acoustics*. Elsevier Inc.

Nilsson, A.C. (1972). *Reduction index and boundary conditions for a wall between two rectangular rooms*. Acustica vol. 26

Sewell, E. C. (1970) *Transmission of reverberant sound through a single-leaf partition surrounded by an infinite rigid baffle*. Journal of Sound and Vibration 12 (1) pp. 21-32.

Smith, P. W. Jr (1964). *Coupling of sound and panel vibration below the critical frequency*. Journal of the Acoustical Society of America 36 (8)

SS 25267:2004, third ed. *Byggnadsakustik – ljudklassning av utrymmen i byggnader – bostäder* (Swedish standard)

Thorsson, P. (2011). Supervision, 2011-04-01.

Acknowledgement

I would like to thank my supervisor Pontus Thorsson for guidance and for suggesting the topic for this thesis. I would also like to thank Krister Larsson for giving me helpful advice concerning the model and the use of Comsol.

At last I would like to thank Professor Wolfgang Kropp and the staff and students at the Division of Applied Acoustics who have helped me in various ways during this period.

Appendix A

```
% Calculate transmission loss
% 'Data' files contain complex vibration velocities from the
% Comsol model



clear all
close all
profile on, profile clear

Nf = 47;                    % number of frequencies
Nai = 32;                   % number of angles for excitation
Nar = 15; Nart=Nar;             % number of angles for radiation
(50okat200Hz
phi = linspace(0,pi/2,Nar); theta = linspace(0,2*pi,Nart);
f = 20*2.^((-1:Nf-2)/6);    % frequency vector

% Constants
c = 343;        % speed of sound
rho = 1.2;      % density of air
rhop = 1300;    % density of plate
h = 0.2;        % thickness of plate
m = rhop*h;     % mass per unit area
E = 3.8e9;      % Young's
D = E*h^3/12;   % bending stiffness

fc = c^2/(2*pi)*sqrt(m/D);    % critical frequency
k = 2*pi*f/c;           % wave number in air
omega = 2*pi*f;               % angular velocity

form = repmat('%f', 1, Nf+2);

% Parameter sweep
for pp=[1 2 3]
    P = zeros(Nf,1);
    Power = zeros(Nf,Nai);
    meanv2 = zeros(Nf,1);
    Pref = zeros(Nf,Nai);

    % Angles of incidence
```

```
    for zz=Nai
        wn = zeros(Nf,1);
        fid =
fopen(strcat('lwc',num2str(pp),'/Data',num2str(zz),'.txt'));
        V = textscan(fid,form,'Headerlines',8);
        fclose(fid);
        % Round x and y koordinates and lengths to milimeter to
        % avoid numerical problems
        xn = V{1,1}; xn = round(1000*xn)/1000;
        yn = V{1,2}; yn = round(1000*yn)/1000;
        a = round(1000*(max(xn)-min(xn)))/1000; % length
        b = round(1000*(max(yn)-min(yn)))/1000; % width
        r = a/b;                                % aspect ratio
        S = a*b;                                % plate surface area
        xn = 2*xn/a; yn = 2*yn/b;

        % Frequencies
        for ii=1:Nf
            if f(ii)<fc
                sl = c/fc/6;
            else sl=(D/m)^(1/4)*sqrt(2*pi)./sqrt(f(ii));
            end
            Nx = ceil(a/sl); Ny = ceil(b/sl);
            % Number of nodes Nx and Ny must be odd!!!
            if mod(Nx,2)==0
                Nx = Nx+1;
            end
            if mod(Ny,2)==0
                Ny=Ny+1;
            end

            % ------------ Weights for numerical integration --------
            hx = 2/(Nx-1);
            x = -1:hx:1;
            wx   =   ones(1,Nx);   wx(2:2:Nx-1)=4;   wx(3:2:Nx-2)=2;
            wx=wx*hx/3;

            hy = 2/(Ny-1);
            y = -1:hy:1;
            wy   =   ones(1,Ny);   wy(2:2:Ny-1)=4;   wy(3:2:Ny-2)=2;
            wy=wy*hy/3;
```

```
[Wx,Wy] = meshgrid(wx,wy);
W = Wx.*Wy;


hp = pi/2/(Nar-1);
wp  =  ones(1,Nar);  wp(2:2:Nar-1)=4;  wp(3:2:Nar-2)=2;
wp=wp*hp/3;


ht = 2*pi/(Nart-1);
wt  =  ones(1,Nart);  wt(2:2:Nart-1)=4;  wt(3:2:Nart-2)=2;
wt=wt*ht/3;
%------------------ Nodal velocities ---------------
zn = V{1,2+ii};
% Sort velocity data from triangular element nodes to
% unique
% coordinates
[~,I,~] = unique([xn yn],'rows');
M = [xn yn zn]; M=M(I,:);


%------------------- Create rectangular mesh----------
% Interpolated real part of velocity
Freal = TriScatteredInterp(M(:,[1 2]),real(M(:,3)));
% Interpolated imaginary part of velocity
Fimag = TriScatteredInterp(M(:,[1 2]),imag(M(:,3)));
[X,Y] = meshgrid(x,y);
% Complex velocity at points of above defined grid
Z = Freal(X,Y)+1i*Fimag(X,Y);

% Preallocating and "cleaning up"
zwn2 = zeros(Nar,1);
Pf = 0;

% Wave number spectrum and calculation of radiated power
for jj=1:Nar
    for kk=1:Nart
        % wave numbers
        kx = k(ii)*sin(phi(jj))*cos(theta(kk));
        ky = k(ii)*sin(phi(jj))*sin(theta(kk));
        % wave number transform zwn2=z(kx,ky)^2

      zvwn=a^2/(4*r)*Z.*exp(1i*(a/2*kx*X)).*exp(1i*(b/2*k
      y*Y)).*W;
        zwn2 = abs(sum(zvwn(:)))^2;
```

```
                    Pf = Pf + rho*omega(ii)^2/ (8*c*pi^2)*zwn2
                  *sin(phi(jj))*wp(jj)*wt(kk); %*4 för 2pi
                end
            end
             % Frequency dependent radiation power and squared
            % mean velocity
            P(ii) = Pf;
            Mv2 = abs(Z).^2.*W/2;
            meanv2(ii) = sum(Mv2(:))/4;
        end
        Power(:,zz) = P;
        Pref(:,zz) = S*rho*c*meanv2;
    end
    filename = strcat('ps',num2str(Nar));
    save(filename,'Power','Pref');
end

profile report, profile off
```

Appendix B

```
% Average transmission coefficient tao for 32 angles of
incidence


clear all

clc

close all


f = 20*2.^((-1:45)/6); Nf = length(f); %Number of frequencies

ft = ters(20,3150);  Nft = length(ft); %third octaves

Nai = 32;       % Number of angles for excitation

Nbc = 22;       % number of boundary conditions

TL    =    zeros(Nft,Nbc);    Rw=zeros(Nbc,9);    C=zeros(Nbc,8);
Pref0=zeros(Nf,Nbc);

RE = zeros(Nft,Nbc); RE6 =zeros(Nf,Nbc);



for ii=1:10   % parameter sweep

    eval(['load' ' lwc' num2str(ii)]);

    tao = gettao_1d(Power);

    TL(:,ii) = -10*log10(tao);

    RE6(:,ii) = mean(Power./Pref,2);

    RE(:,ii) = 10*log10(tersgen(RE6(:,ii)));

    [Rw0,~,~,C0] = rweight(ft(5:end),TL(5:end,ii)');

    Rw(ii,:) = [Rw0 C0];

end
```

Appendix C

```
% Calculate tranmission coefficient tao from radiated power
%vector "Power"

function tao = gettao_1d(Power)
S = 2.6*4.2;    % surface area of wall
Na = length(Power(1,:));    % number of incidence angles
phi = linspace(0,1.36,Na);
p = 1/2;                    % pressure amplitude
I = p^2/(2*343*1.2)*S;      % incident power "amplitude"
Pin = I*mean(cos(phi));
P = mean(Power,2);
P = tersgen(P);
tao = P/Pin;
```